Origin of seismic repeaters in a deep mine: what do we learn from in-situ investigation coupling geology, geomechanics and geophysics?

Emeline Lhoumaud
GeoRessources lab, Université de Lorraine - CNRS, Mines Nancy, Campus ARTEM, BP14234, Nancy, France

Yann Gunzburger
GeoRessources lab, Université de Lorraine - CNRS, Mines Nancy, Campus ARTEM, BP14234, Nancy, France

Marianne Conin
GeoRessources lab, Université de Lorraine - CNRS, Mines Nancy, Campus ARTEM, BP14234, Nancy, France

Jannes Kinscher
Institut National de l'Environnement Industriel et des Risques (INERIS), Campus ARTEM CS14234, Nancy Cedex, France

ABSTRACT: Seismic repeaters (i.e. seismic events with highly similar waveforms) have been observed in the deep mine of Garpenberg, Sweden. In natural seismology, repeaters are commonly associated with the presence of aseismic slip (i.e. creep) on fault planes, loading seismogenic asperities. This raises questions regarding what these asperities and creeping zone consist of and how they behave from a mechanical point of view. A local monitoring network has been installed in situ, close to the source area of one family of repeaters at 1km depth, with the objective of identifying the origin of these repeaters. The network comprises boreholes, geophones and strain cells. We show that the presence of a fault plane with creeping portions and an asperity is compatible with field data. We also discuss the difficulty of clearly identifying the origin of the repeaters, as we couldn't reach the seismic asperity itself, even with such a local network.

Keywords: Induced seismicity, seismic repeaters, deep mining, in-situ investigation.

1 INTRODUCTION

1.1 Type area and previous analyses

The Garpenberg mine is located in central Sweden and is exploited by Boliden mining company. It is composed by several vertical massive sulphides lenses, hosted by altered and metamorphosed felsic volcanic rocks and limestone (Tiu et al., 2021). The orebody of Lappberget is the largest in the mine (De Santis et al., 2019). It is cut by several shear zones, parallel to the orebody and associated with talc and chlorite. The area of our study is located within a sill-pillar at 1km depth, just above the panel of excavation block 1250 (see Figure 1). The mainly-used mining method is sublevel stoping.

Kinscher et al. (2020) highlighted the presence of 17 families of repeaters within the block 1250 and the sill-pillar ($-2.5 < Mw < 1$, on moment magnitude scale). Repeaters are well-known in natural seismology. They have been for example intensively studied on the San-Andreas fault (Nadeau et al., 1995) and on the North Anatolian fault (Uchida, 2019). They are commonly associated with the

presence of the seismogenic breaking of asperities loaded by aseismic slip within weak material filled fault planes (Carpenter et al., 2011; Chen & Lapusta, 2009; Dieterich, 1992).

Source mechanisms of the repeaters show a strike-slip movement with a reverse component. Their sources align along horizontal directions parallel to the stopes (Y axis) and are reactivated over long periods of time (from several days up to several years). Magnitudes range between -2 and 1, at the moment scale magnitude. Kinscher et al. (2020) suggest repeaters are triggered by fractures filled with weak-material like talc, loading asperities of a few meters size. To identify the origin of these repeaters more precisely, we focused on one specific family (Table 1) located within the sill-pillar, accessible from mine drifts. We aim at reaching the structure at the origin of the repeaters and study its characteristics.

Table 1. Characteristics of the nodal plane of target family of repeaters given by seismic analyses. The nodal plane is deduced from the seismic source mechanism and events location.

Strike	Dip	Rake	Source mechanism	Mw average	Slip average
190°	75°	130°	strike-slip with reverse component	-0,3	1mm

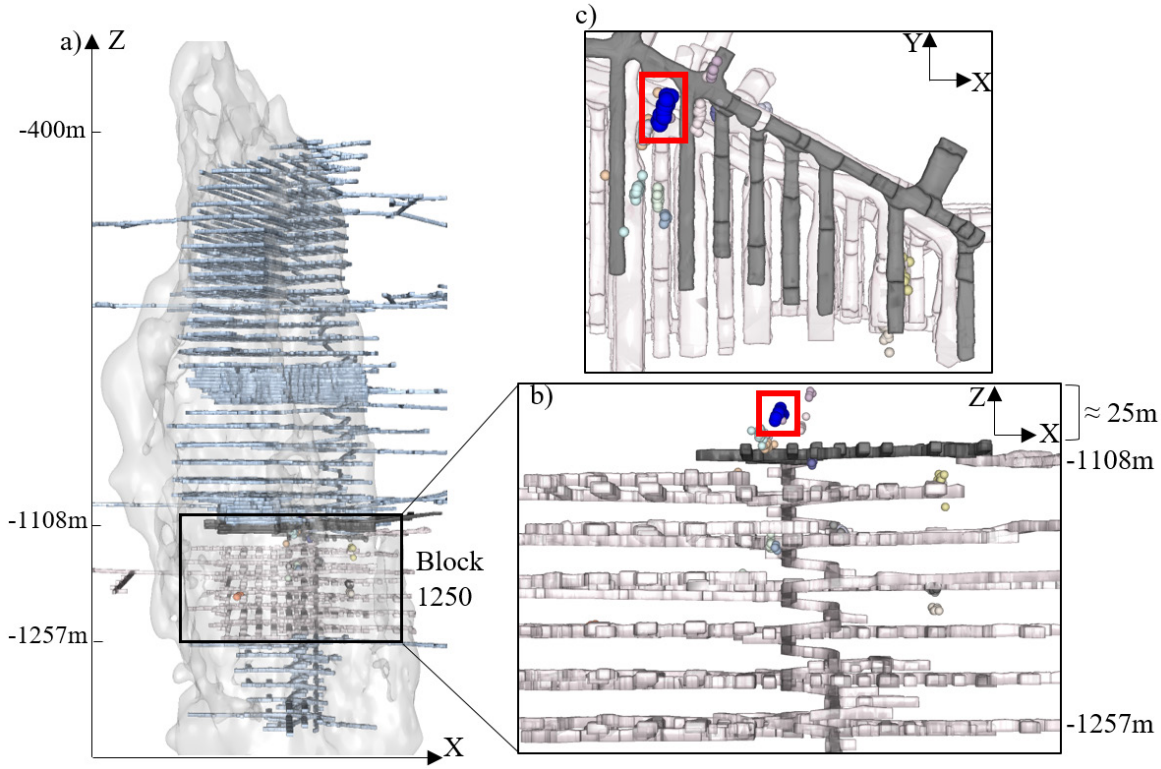

Figure 1. (a) Vertical view of the orebody of Lappberget and (b) a zoom of the area of monitoring of Ineris since 2015. Spheres of different colors represent the 17th families of repeaters detected by the previous network. Upper right image (c) is a plane view of the monitored area and shows the alignment of the families along Y-axis direction. Red square indicates the family of repeaters described in table 1, which is the target family of our study, located in the sill-pillar of the area.

1.2 Local installation

Several boreholes with different orientations and inclinations were drilled to reach the source of the repeaters family and compare field data with what is usually observed in presence of repeaters in seismology (see Figure 2). Four CSIRO Hi12 strain cells were installed in the boreholes. Each of them comprises 12 gauges and records strains every minute. The installation is located between the

orebody (siliceous rocks with different types of micas) and the hosting rocks (sedimentary and marble rocks), which are lithologies commonly observed elsewhere in the mine.

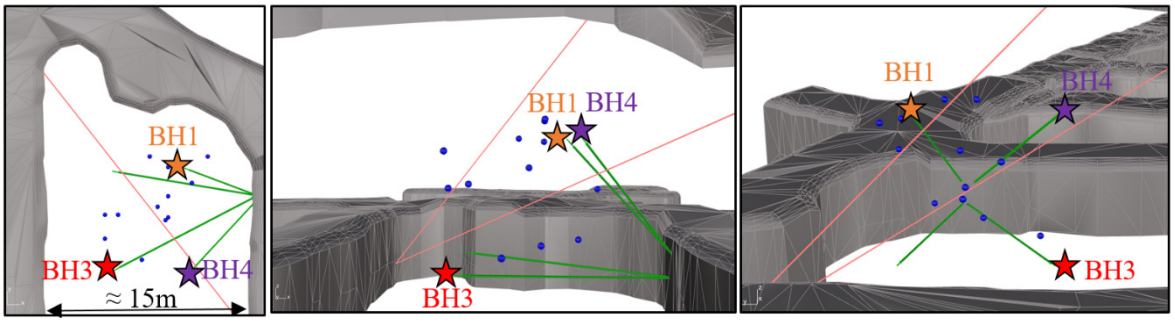

Figure 2. Local installation within the sill-pillar. Events of the target family are showed in blue spheres. Colored stars and green lines represent the strain cells and their associated drillings. Red lines show two additional drillings for lithological and fracturation information. Upper and below drifts of excavation of the sill-pillar are represented in grey.

2 DATA ANALYSES

2.1 Drill cores analysis

The orientations of the fractures in the cores have been measured using the method of Holcombe (2013). Only one family of fractures has an orientation compatible with the orientation of the target fault plane given by the seismic analyses (Figure 3). X-ray diffraction (XRD) shows that these fractures contain muscovite and chlorite infilling. Chlorite has a low coefficient of friction (Ikari et al., 2009), which suggests it may slip aseismically. Therefore, similarly to what is known from natural seismology, we can assume the boreholes have intersected the aseismic part of the fault plane at the origin of the repeaters. The locked part of the fault with higher coefficient of friction (i.e. seismic asperity), loaded by this aseismic slip and breaking repetitively, is unknown.

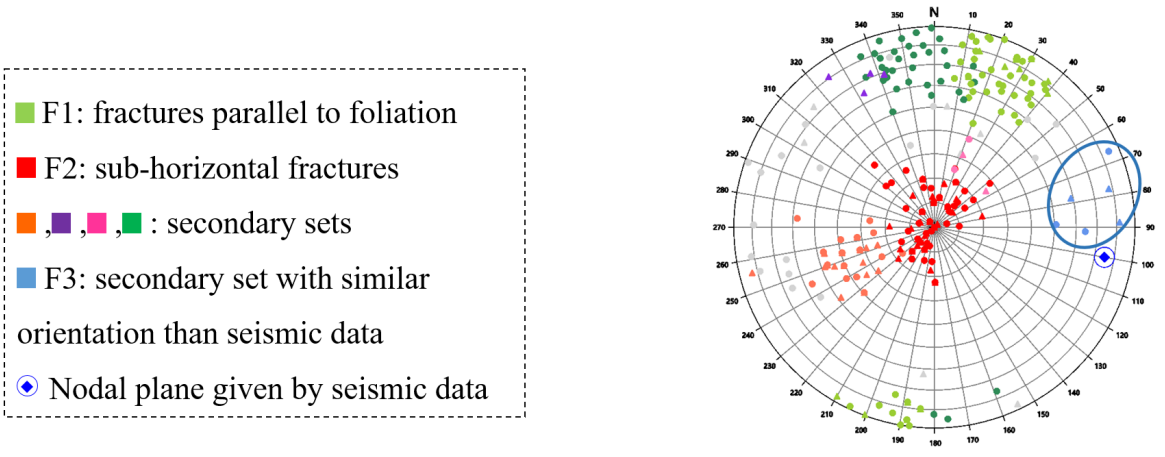

Figure 3. Orientation of the fractures in the drill cores. Main families are F1 and F2 families, highly represented in the drill cores. Blue circle represents the only secondary family with orientation compatible with the seismic nodal plane given by previous seismic analyses.

2.2 Strain monitoring

An instantaneous co-seismic shift of deformation of around 6 microstrains (με) was monitored by the strain cell BH4 during a seismic event of magnitude M=-1. This event is an order of magnitude higher than the other events monitored during the eight months of observation, which explains why it has been detected. The immediate response is visible on the cell recordings and we have calculated the strain tensor associated with this event (Amadei & Stephansson, 1997; Worotnicki, 1993). The three principal strains are shown in Figure 4.

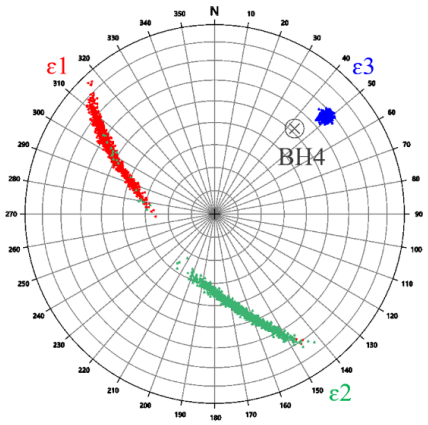

Figure 4. Principal strains during the co-seismic shift of deformation. Dots represent incertitude on the orientations. Values are ε3=-6,6με (extension), ε2 = +0,96με (shortening), ε1 = +1,7με (shortening). The deformation occurs mainly as an extension (ε3) in the drilling direction (BH4).

3 EVALUATION OF THE PRESENCE OF AN ASEISMIC/SEISMIC COUPLED FAULT PLANE

3.1 Location of the seismogenic asperity

Strain data were used, along with Okada's model (Okada, 1992) to locate the seismic asperity, using an inverse-problem approach. With Okada's model, the strain tensors induced by a rectangular dislocation within an elastic and isotropic medium can be calculated analytically. We computed the induced strains for different possible locations of the asperity, within a radius of 10 meters around the location of the seismic event of the 18th of January given by seismic analyses (based on location error). The size of the asperity in the model ranges between 1 and 10 meters. For each location of the dislocation, strain tensors are computed at the location of the strain cells and compared with strain measurements. Computed and measured strains are considered as compatible if the signs are the same, if strain mainly occurs along the extensive component (ε3) and if the orientations of principal strains are within the uncertainty range of the strain cells. Modeled and BH3/BH1 cells are compatible if their values are considered sufficiently small not to be detected by the cells.

Doing so, we identified two clusters of possible locations for the seismic asperity (Figure 5). Both are outside the area reached by the drillings. The area located to west is generally closer to the seismic event location and we show a possible location for the asperity within the cluster. The chosen asperity has a size of 3m x 3m and is at 6 m from the location given by seismic analysis, which is consistent with the location error.

3.2 Aseismic/seismic fault plane

We consider that the asperity is part of a fault plane slipping aseismically, as commonly described in seismology. Dimensions of the plane are unknown but we consider the plane large enough to be reached by the drillings. The orientation is assumed to be the same as that given by seismic analyses.

One drilling intersects the plane where most of F3 fractures (oriented similarly to the seismic nodal plane and with chlorite infilling) have been observed in the drill cores. This shows an excellent agreement between geophysical, geological and geomechanical data.

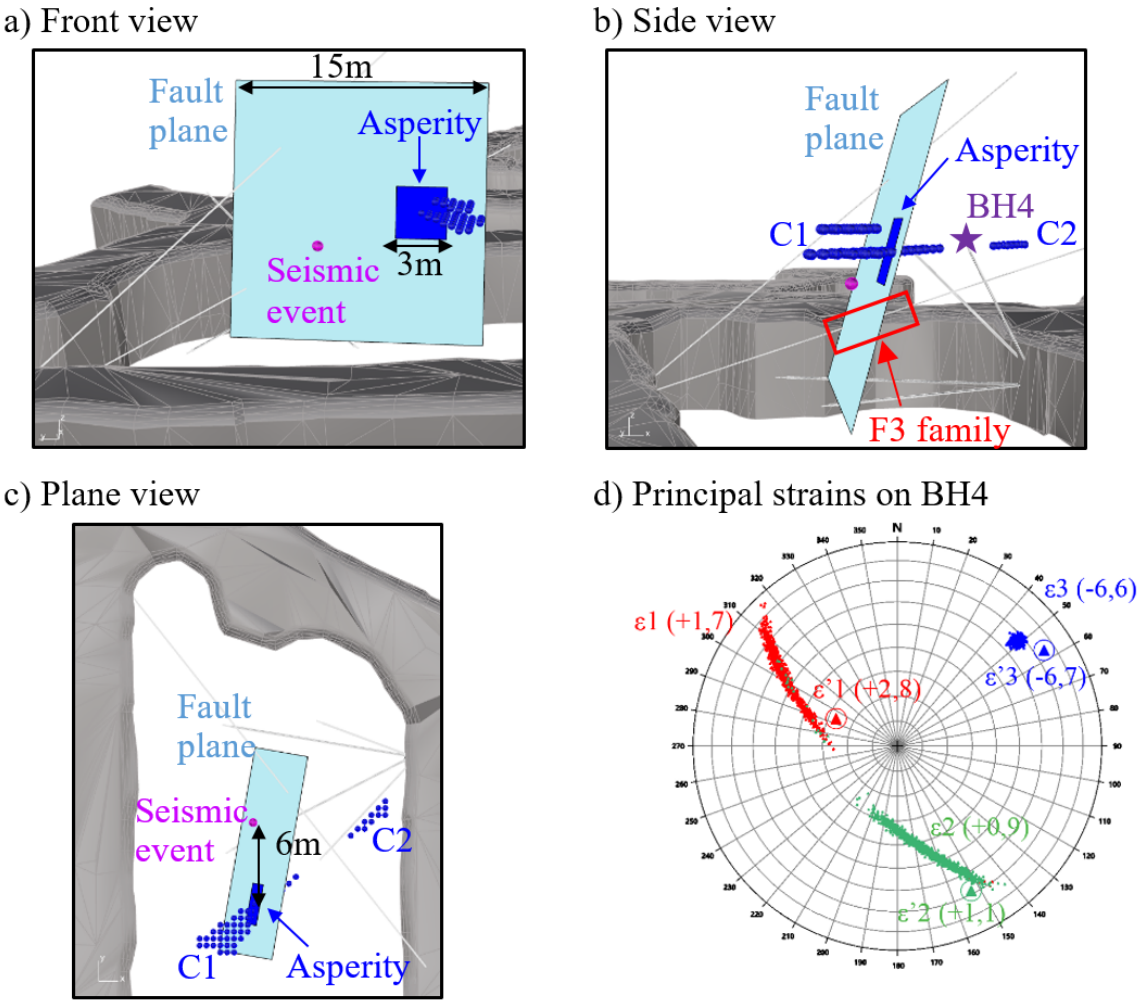

Figure 5. Localization of one possible fault plane responsible of the monitored seismicity with one asperity. Blue spheres represent two clusters C1 and C2 of possible localizations of the asperity, determined from both seismic and strain data. One asperity has been chosen and is showed in dark blue. The asperity is located at 6meters from the seismic event (purple sphere). The asperity is assumed to be located on an aseismically slipping fault (light blue) with similar orientation. This fault plane crosses the drillings where F3 fractures have been observed in the drill cores. Slip on the asperity simulated with Okada model gives strain values compatible with BH4 cell.

CONCLUSION

The studied area represents an incredible opportunity to investigate the origin of seismic repeaters in a deep mine. We show seismic repeaters in the monitored area can be triggered by the presence of a fault plane entailing aseismic portions and at least one asperity, as commonly observed in natural seismology. Drillings crossed a family of fractures with a weak-material infilling and with an orientation similar to the seismic nodal plane, which might correspond to the aseismic portion of the fault plane. The seismic asperity was not observed in the drillings but strain cells allowed us to locate it outside the area reached by the drillings but not far away. Our model also shows that a size of the asperity between 1-10 m, as given by as seismic analysis, give strain measurements consistent with

what is monitored. Further investigations are needed to actually conclude on the origin of these repeaters. One option would be to drill in the clusters of new constrained locations of the asperity to try to reach it. If successful, we would have access to both seismic and aseismic portions of the plane, which will represent an incredible opportunity to study the behavior of such a fault plane.

REFERENCES

Amadei, B., & Stephansson, O. (1997). *Rock stress and its measurement* (Chapman and Hall (ed.); pp. 201–276).

Carpenter, B. M., Marone, C., & Saffer, D. M. (2011). Weakness of the San Andreas Fault revealed by samples from the active fault zone. *Nature Geoscience*, *4*(4), 251–254. https://doi.org/10.1038/ngeo1089

Chen, T., & Lapusta, N. (2009). Scaling of small repeating earthquakes explained by interaction of seismic and aseismic slip in a rate and state fault model. *Journal of Geophysical Research: Solid Earth*, *114*(1), 1–12. https://doi.org/10.1029/2008JB005749

De Santis, F., Contrucci, I., Kinscher, J., Bernard, P., Renaud, V., & Gunzburger, Y. (2019). Impact of Geological Heterogeneities on Induced-Seismicity in a Deep Sublevel Stoping Mine. *Pure and Applied Geophysics*, *176*(2), 697–717. https://doi.org/10.1007/s00024-018-2020-9

Dieterich, J. H. (1992). Earthquake nucleation on faults with rate-and state-dependent strength. *Tectonophysics*, *211*, 115–134.

Holcombe, R. (2013). Oriented drillcore: measurement, conversion, and qa/qc procedures for structural and exploration geologists (Issue May).

Ikari, M. J., Saffer, D. M., & Marone, C. (2009). Frictional and hydrologic properties of clay-rich fault gouge. *Journal of Geophysical Research: Solid Earth*, *114*(5), 1–18. https://doi.org/10.1029/2008JB006089

Kinscher, J. L., De Santis, F., Poiata, N., Bernard, P., Palgunadi, K. H., & Contrucci, I. (2020). Seismic repeaters linked to weak rock-mass creep in deep excavation mining. *Geophysical Journal International*, *222*(1), 110–131. https://doi.org/10.1093/gji/ggaa150

Nadeau, R. M., Foxall, W., & McEvilly, T. V. (1995). Clustering and periodic recurrence of microearthquakes on the San Andreas fault at Parkfield, California. *Science*, *267*(5197), 503–507. https://doi.org/10.1126/science.267.5197.503

Okada, Y. (1992). Internal deformation due to shear and tensile faults in a half-space. *Bulletin - Seismological Society of America*, *82*(2), 1018–1040. https://doi.org/10.1785/bssa0820021018

Tiu, G., Jansson, N., Wanhainen, C., Ghorbani, Y., & Lilja, L. (2021). Ore mineralogy and trace element (re)distribution at the metamorphosed Lappberget Zn-Pb-Ag-(Cu-Au) deposit, Garpenberg, Sweden. *Ore Geology Reviews*, 104223. https://doi.org/10.1016/j.oregeorev.2021.104223

Uchida, N. (2019). Detection of repeating earthquakes and their application in characterizing slow fault slip. *Progress in Earth and Planetary Science*, *6*(1). https://doi.org/10.1186/s40645-019-0284-z

Worotnicki, G. (1993). Csiro Triaxial Stress Measurement Cell. In J. A. Hudson (Ed.), *Comprehensive rock engineering* (pp. 329–394). Pergamon Press Ltd, Oxford.